Catalysis Communications 114 (2018) 19–23

Contents lists available at ScienceDirect

Catalysis Communications

journal homepage: www.elsevier.com/locate/catcom

Short communication

Catalytic behavior of Ru nanoparticles supported on carbon fibers for the ethanol steam reforming reaction

María Laura Bosko[a], Nicolás Ferreira[a], Antonella Catena[a], M. Sergio Moreno[b], John F. Múnera[a,*], Laura Cornaglia[a]

[a] Instituto de Investigaciones en Catálisis y Petroquímica, Universidad Nacional del Litoral, CONICET, Facultad de Ingeniería Química, Santiago del Estero 2829, 3000 Santa Fe, Argentina.
[b] Centro Atómico Bariloche, 8400 S. C. de Bariloche, Argentina.

ARTICLE INFO

Keywords:
Ru catalysts
Ethanol steam reforming
Carbon fibers
Electroless deposition

ABSTRACT

Ru catalysts on carbon fibers were prepared by electroless deposition, with 0.6 wt% Ru loading. The reduced and used catalysts were characterized by different techniques in order to analyze oxidation states and surface composition, the metallic content at volumetric level, and particle size. These solids were evaluated for the production of hydrogen via ethanol steam reforming at different gas hour space velocities (GHSV) at 723 K. Space velocity significantly influenced the distribution of products favoring the formation of acetaldehyde at short contact times while, for longer times, it was possible to obtain a hydrogen rich stream, free of oxygenate compounds.

1. Introduction

Because to environmental concerns and the limited availability of fossil fuels, renewable sources of energy are increasingly investigated worldwide. Within this perspective, hydrogen is a very interesting alternative to be used in fuel cells when it is obtained from ethanol steam reforming (ESR). However, this reaction takes place simultaneously with a number of side reactions leading to the production of CO, acetaldehyde and methane. Therefore, it is necessary to have an active, stable and hydrogen selective catalyst.

Ethanol steam reforming

$$CH_3CH_2OH + 3H_2O \Leftrightarrow 6H_2 + 2CO_2 \quad (1)$$

Ethanol decomposition

$$CH_3CH_2OH \Leftrightarrow CH_4 + CO + H_2 \quad (2)$$

Methane steam reforming

$$CH_4 + H_2O \Leftrightarrow 3H_2 + CO \quad (3)$$

Water *gas* shift

$$CO + H_2O \Leftrightarrow H_2 + CO_2 \quad (4)$$

Ethanol dehydrogenation

$$CH_3CH_2OH \Leftrightarrow H_2 + CH_3CHO \quad (5)$$

Acetaldehyde decomposition

$$CH_3CHO \Leftrightarrow CH_4 + CO \quad (6)$$

In this context, several reports [1–3] have been published in which the active phase is supported on high surface area oxides (silica, alumina and CeO_2). A drawback of the use of these supports is their reactivity, which can cause a strong interaction with the active metal, forming a hardly reducible compound. The application of inert supports made from carbon-based materials with high specific area and thermal stability, can solve this problem [4,5]. On the other hand, carbon fibers as substrates have several advantages over other materials because they can reduce diffusion limitations and pressure drop in the reactors. These fibers also combine an open macro structure with mechanical flexibility [6].

Among the metals used as active phases in the ESR, Rh and Ru are known to successfully break the C—C bond leading to less coke deposition and more stable catalysts [7]. In a previous work [8] we reported stable $Rh/La_2O_3SiO_2$ catalysts with high activity and H_2 selectivity employing low metal content (0.6 wt%). Liguras et al. [7] found that Rh was significantly more active and selective towards hydrogen formation than Ru and Pt. However, the authors concluded that the Ru catalyst performance was greatly improved by increasing the metal loading (5 wt%). Therefore, considering the lower cost of Ru if compared with Rh, it is important to study alternative methods of synthesis of Ru catalysts in order to obtain active solids with low metal

* Corresponding author.
E-mail address: jmunera@fiq.unl.edu.ar (J.F. Múnera).

https://doi.org/10.1016/j.catcom.2018.05.019
Received 6 March 2018; Received in revised form 16 May 2018; Accepted 24 May 2018
Available online 27 May 2018
1566-7367/

loading.

Incipient wetness and wet impregnations [9–11] are usually selected as synthesis methods to prepare noble metal catalysts for reforming reactions. At present, the electroless deposition (ED) technique is considered as a feasible alternative for the deposition of metallic nanoparticles on various substrates [12]. With the purpose of finding active, stable and selective catalysts for the ESR, this work reports the use of Ru-based catalyst supported on carbon fibers prepared by ED. The reduced and used samples were characterized by several characterization techniques in order to study the metal particle sizes, surface oxidation states and bulk composition.

2. Experimental

2.1. Catalyst preparation

Commercial activated carbon felts (ACN 211-15) were employed as supports. They were purchased from American Technical Trading, Inc. The substrate was cut in rounded pieces (Ø = 8 mm) before the preparation of the catalysts. The felts were pre-treated in an acidic aqueous solution of HCl 4.8 M for 2 h at 323 K to eliminate inorganic impurities [12] and then rinsed in distilled water and dried at 353 K overnight. The carbon felt density was estimated from the weight (180 g m^{-2}) and thickness (2 mm) data, provided by the manufacturer.

Electroless deposition was employed to deposit Ru nanoparticles with a controlled deposition rate. Using this technique, Ru nanoparticles were produced and deposited on the substrate surface via a redox reaction between the complex ion of reducible metal and the reductant. The complex solution was prepared from $RuCl_3.xH_2O$ (Alfa Aesar, 99.9%) as precursor salt and two complexing agents, $NaNO_2$ and NH_4OH. Firstly, the metal precursor was dissolved in distilled water, and then the sodium nitrite was added. Latter the solution was heated to 370 K and the ammonium hydroxide was incorporated. The felts were immersed into the deposition bath with ultrasound assistance (40 kHz) at 308 K for 90 min where hydrazine as reducing agent was gradually added in eight portions (12.5 mL L^{-1}) every 10 min. Finally, the solids were carefully rinsed with deionized water and then dried at 353 K. The ED bath composition is shown in Table 1. Ru deposition efficiency was estimated around 2%.

The Ru content of the prepared catalysts was measured by XRF (X-Ray Fluorescence). The value obtained was 0.6 wt%. The BET surface area of the support was 1020 $m^2 g^{-1}$ after being exposed to the synthesis steps with a Ru free solution. Prior to the characterization, the catalysts were reduced in H_2 flow at 673 K during 2 h.

2.2. Sample characterization

X-ray photoelectron spectroscopy (XPS) analyses were performed in a multi-technique system (SPECS) equipped with a dual Mg/Al X-ray source and a hemispherical PHOIBOS 150 analyzer operated in the fixed analyzer transmission (FAT) mode. The spectra were obtained with a pass energy of 30 eV; a Mg-Kα X-ray source was operated at 200 W and 12 kV.

Scanning Electron Microscopy (SEM) images were obtained using a JEOL scanning electron microscope model JSM-35C. High resolution transmission electron microscopy (HRTEM) images were obtained using a Tecnai F20 G^2 transmission electron microscope, operated at room temperature and 200 kV. EDS was used to analyze the elements present in the different features observed in the HRTEM images.

X-ray Fluorescence analyses were performed employing in a Shimadzu spectrometer, equipped with an energy dispersive system (Model EDX-720) with a high detection range (from Na^{11} to U^{92}), an X-Ray source of Rh, operated at 50 kV and 100 μA, and five X-ray primary filters.

Table 1
Conditions and chemical composition of the ED solution.

	Ru bath
$RuCl_3{\cdot}3H_2O$	1.2
NH_4OH 28–30% (mL L^{-1})	60
$NaNO_2$ (g L^{-1})	1.5
pH	~11
Temperature (K)	308
Solution volume (mL)	50
Fiber mass (mg)	90
Reducing Agent: initial concentration and quantity employed in each solution.	
$N_2H_4{\cdot}H_2O$ (g L^{-1}) initial	12.36
mL solution	5

2.3. Catalytic test

The ethanol steam reforming reaction was carried out in a tubular quartz reactor (i.d. = 6 mm) at 723 K. The catalytic bed (27.9, 39.4 or 50.1 mg of catalyst) was heated up in flowing Ar to the reaction temperature (7 K min^{-1}), and reduced under a H_2 atmosphere for 2 h at the reaction temperature. Next, the water/ethanol mixture (water/ethanol molar ratio = 5) diluted in Ar was fed to the reactor. The inert flow (Ar) was maintained at 60 mL min^{-1} by a mass flow controller. The water/ethanol liquid mixture (0.5 mL h^{-1}) was fed by a syringe pump (Apema PC11U) to an evaporator operating at 493 K. Three different gas hour space velocities (GHSV) were employed (13,006, 9210 and 7243 h^{-1}). All pipes and valves were heated at 453 K to avoid possible condensations. Reactants and reaction products were quantified with a Shimadzu GC-2014 gas chromatograph, equipped with a 10-meter long packed column Hayesep D® and a TCD detector with Ar as carrier gas [8]. C balance was always within ± 5%.

3. Results and discussion

In order to understand the catalyst performance in ethanol steam reforming for hydrogen production, the catalytic materials were characterized and evaluated under different GHSV.

3.1. Morphology of the nanoparticles deposited

The morphology of Ru deposited on the carbon fibers was studied by HRTEM. Fig. 1 shows a fairly uniform distribution of small nanoparticles with a Log Normal distribution. The average size estimated from the fitting of the histogram was 1.4 nm (Fig. 1). We used the Fast Fourier Transform (FFT) of windowed regions in the HRTEM images for the local determination of the phases present in the sample. The region marked by the green square (Fig. 1) illustrates our general observation that only reflections corresponding to ruthenium at 2.34 Å, 2.14 Å and 2.05 Å were observed. The particle diameter estimated by CO chemisorption (1.3 nm) is in agreement concordance with the one obtained by TEM.

3.2. Catalytic performance

With the purpose of verifying the thermal stability of the Ru−C at high temperature, a test with water as only reactant was carried out. Before the test, the catalyst was subjected to the same reduction treatment previously described. In the case of the solid evaluated at 773 K, CO_2 and H_2 were observed in the reactor outlet stream, indicating that the support oxidation/gasification could occur. However, when the experiment was carried out at 723 K, neither CO_2 nor H_2 were detected, making it possible to conclude that at this temperature the presence of a high water concentration does not influence the support stability. In addition, no pressure drop associated with the catalytic bed was detected.

In order to test the catalyst performance, experiments varying space

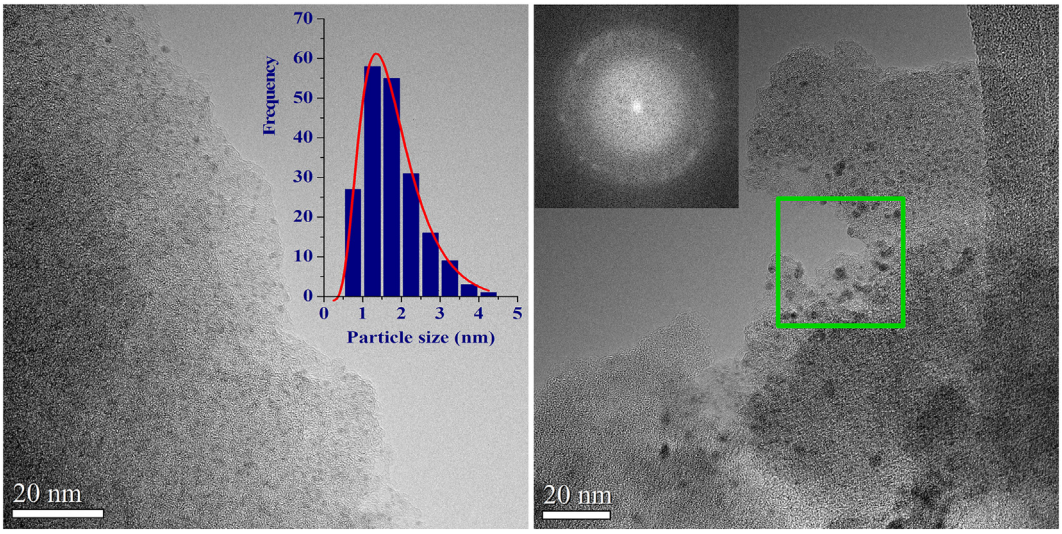

Fig. 1. HRTEM image of the tip of a carbon fiber of Ru−C sample. The right inset shows the FFT of nanoparticles in the region with the green square; and the left one displays the histogram of the Ru nanoparticle size distributions. The solid line is a fitting with a Log Norm function. (For interpretation of the references to colour in this figure legend, the reader is referred to the web version of this article.)

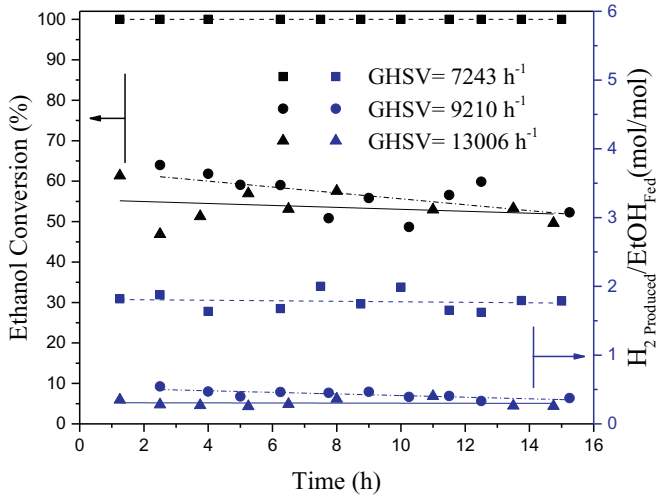

Fig. 2. Ru−C fibers conversion and hydrogen yield in ethanol steam reforming, evaluated at different space velocities. Water/Ethanol molar relation = 5. T = 723 K. Equilibrium conversion = 100%, equilibrium H_2 yield = 3.26. Estimated by STANJAN.

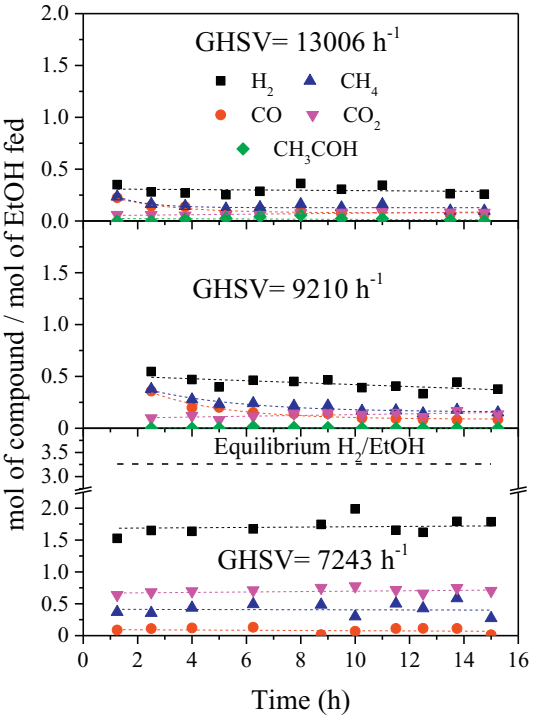

Fig. 3. Ru−C fibers product distribution in ethanol steam reforming, evaluated at different space velocities. Water/Ethanol molar relation = 5. T = 723 K.

velocity were carried out at 723 K (Fig. 2). No significant differences were observed between the two higher space velocities in terms of conversion and hydrogen production. For GHSV = 7243 h^{-1}, the influence of space velocity could be clearly observed by comparing H_2 produced/ethanol feed ratio. This value was practically 3 times higher than the one obtained for the other two GHSV. This behavior agrees with the ethanol conversion results, showing not only high activity, but also good selectivity towards H_2, when decreasing the space velocity. It is important to note that there are not many reports in the literature about the stability of the catalysts at low temperature. Bilial et al. [13] investigated long term stability of Ru(0.2 wt%)/Al_2O_3 at higher temperature (773 K) with a GHSV of 50,000 h^{-1} achieving total ethanol conversion during the first 6 h; afterwards, conversion remained around 70% for the following 90 h on stream.

Note that for comparison purposes, Fig. 2 only shows the stability during 15 h on stream for all the measured space velocities. However, at the lowest space velocity, the catalyst exhibited complete ethanol conversion for more than 40 h under reaction conditions (Supplementary material).

The ratio of compound produced by ethanol fed for all space velocities is shown in Fig. 3. It can be observed that the highest H_2 production was obtained for GHSV = 7243 h^{-1}. No less important is the low formation of carbon monoxide under these operating conditions.

Analyzing the product distribution at the high GHSV shown in Fig. 3, the presence of acetaldehyde would be indicating out that the ethanol dehydrogenation (5) is taking place. This is to be expected considering that ESR (1) is favored at temperatures above 823 K and ethanol decomposition (2) and dehydrogenation (5) occur at lower temperatures [1,14]. However, the small amount of acetaldehyde and the high concentration of methane suggest that the catalyst exhibits a

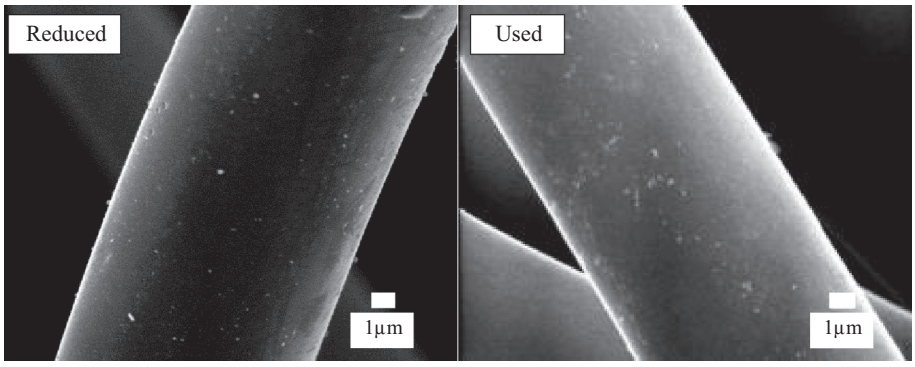

Fig. 4. SEM micrographs of the reduced and used Ru−C catalyst at 723 K and GHSV 7243 h^{-1} during 44 h.

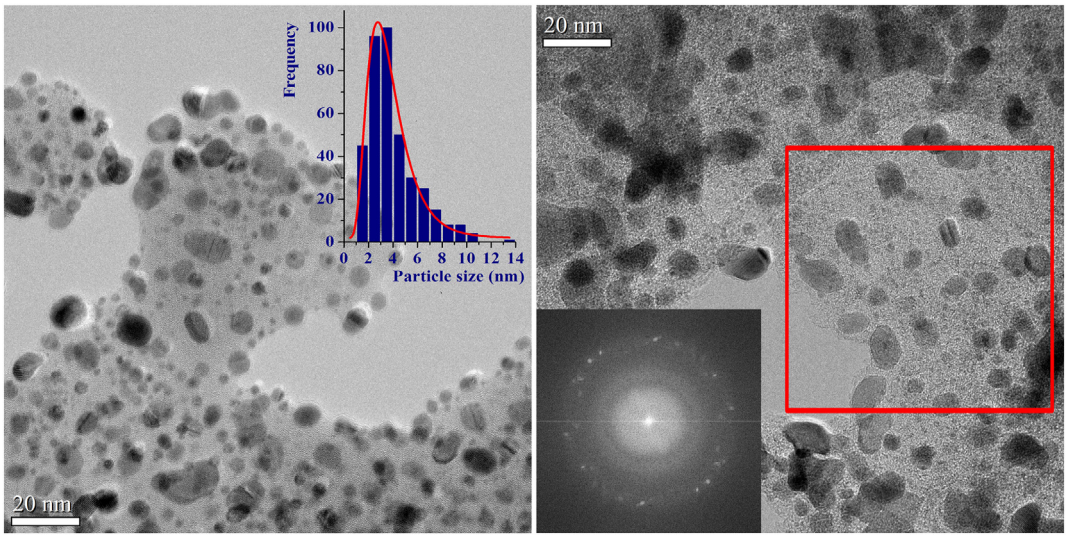

Fig. 5. HRTEM image of the tip of a carbon fiber of used Ru−C catalyst at 723 K and GHSV 7243 h^{-1} during 44 h. The right inset shows the FFT of nanoparticles in the marked region in red; the left one displays the histogram of the particle size distribution. The solid line is a fitting with a Log Norm function. (For interpretation of the references to colour in this figure legend, the reader is referred to the web version of this article.)

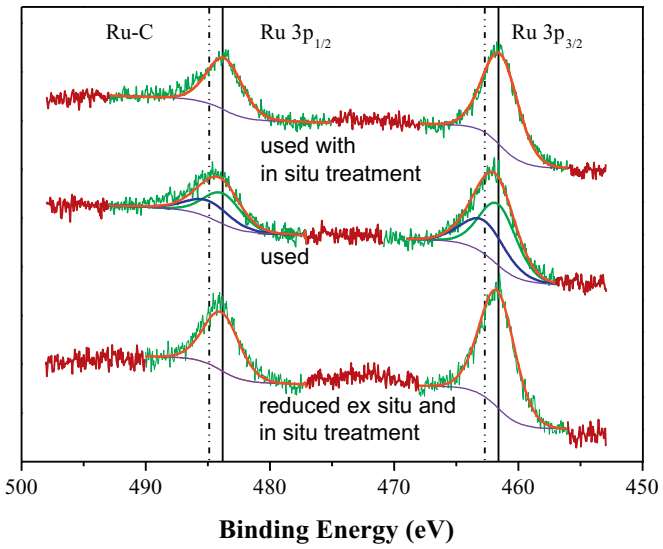

Fig. 6. Ru 3p core level spectra for the Ru−C catalyst on different conditions. Ex situ reduction: the solid was previously reduced (external oven) in H_2 flow at 673 K, 2 h. Used Ru−C catalyst at 723 K and GHSV 7243 h^{-1} during 44 h. In situ treatment: the catalyst was reduced in the spectrometer reaction chamber at 673 K, 10 min with a 5% H_2/Ar flow.

higher selectivity towards ethanol decomposition, which is in agreement with the results on noble metal based catalysts reported in the literature [2].

The decrease in the CO composition in the product stream as well as the increasing concentration of H_2 and CO_2 when the GHSV decreased to 7243 h^{-1} indicates that the WGS reaction (4) is likely to happen. This is in agreement with the results reported by Mudiyanselage et al. [15] who claimed that water gas shift (WGS) reaction was favored on Ru(0.5 wt%)/CeO_2 at low temperatures, leading to an increase in H_2 production. It can also be noted that no acetaldehyde was detected. This behavior suggests its further decomposition to CO and methane (6), showing its role as an intermediate species in the reaction process. This tendency is in agreement with some authors [16] who observed an increment in ethanol conversion as GHSV decreased. However, in this case, it can be noted that total ethanol conversion followed complete acetaldehyde decomposition, as well as methane reforming and CO further reaction (3,4), enlarging hydrogen selectivity which can be identified in the product distribution. Compagnoni et al. [17] reported a similar behavior, indicating a decay in acetaldehyde and ethylene selectivity with the decrease of the GHSV.

3.3. Characterization of the used solid at GHSV = 7243 h^{-1}

Characterization analyses were used as a starting point for understanding the performance aspects of our catalyst. The Raman spectra (Supplementary material) of the structured catalyst before and after the

reaction at 723 K and GHSV of 7243 h^{-1} during 44 h were similar, showing two main signals: the band at 1600 cm^{-1} was attributed to the stretching mode of the graphitic lattice (E_{2g} symmetry), while the band at 1335 cm^{-1} was associated of structural network disorder.

The SEM images of the reduced Ru−C catalyst show the typical morphology of the carbon fibers; with diameters between 10 and 15 μm with a cross-linked 3D structure (Fig. 4). After exposure to the reaction conditions the structure of the fibers did not change (Supplementary material). These results could be associated with the high stability observed in the catalyst during more than 40 h. By analyzing the ruthenium particle sizes (Fig. 5), it can be seen that the exposure to ESR increased the mean size to 2.8 nm with a similar distribution. Nevertheless, this change was practically not reflected in the catalytic behavior. On the other hand, the FFTs revealed reflections corresponding to metallic ruthenium. However, after a careful inspection of the sample, we found very few nanoparticles of RuO_2. Note that, the ruthenium oxide nanoparticles were observed only in the used solid; suggesting that metallic particles could be oxidized during the reaction.

Finally, in order to obtain a relationship between the nature of the metallic phase and the catalytic performance, XPS measurements were carried out in the Ru 3p region. The Ru−C spectra after different treatments are shown in Fig. 6. The plots present the characteristic Ru doublets $3p_{1/2} - 3p_{3/2}$, with a separation of 22.2 eV for all samples. When they were reduced in situ (reduced and used for 44 h), with a short treatment of 10 min at 673 K in hydrogen atmosphere (5%), a single peak was observed at 461.6 ± 0.1 eV corresponding to Ru^0 [18–20] with FWHM of 3.4 eV. This implies that the metallic ruthenium could be available during the reaction when hydrogen is present. From the spectra of the used sample (exposed to air) two signals in each doublet are displayed; the signal at higher BE (462.7 eV) with a 39% contribution can be assigned to Ru oxidized species [18–22]. The same behavior was observed in the sample reduced ex situ and exposed to ambient conditions. Therefore, the presence of Ru^{n+} signals could be assigned to exposure to air as well as to reaction conditions; in agreement with the TEM results. On the other hand, the Ru/C atomic ratios of the reduced and used catalysts were equal to 3.8 and 2.9 suggesting that no significant sintering of the ruthenium particles was produced during the ESR.

4. Conclusions

Ru solids (0.6 wt%) supported on carbon fibers were synthesized by electroless deposition. The selected technique was adequate to nanoparticle deposition over this substrate. The TEM images of the reduced catalyst showed Ru nanoparticles with an average size of 1.4 nm. After the exposure to ESR, the mean size was slightly increased to 2.8 nm and a minor fraction of RuO_2 nanoparticles was found. In agreement, the XPS analysis also suggested that the dispersion of Ru nanoparticles did not significantly change.

Ru nanoparticles supported on a structured substrate were applied in the ethanol steam reforming reaction at 723 K. High ethanol conversion was obtained during 44 h in reaction. Besides, at high contact times, a hydrogen-rich stream free of oxygenated compounds and with low carbon monoxide content was obtained.

Acknowledgments

The authors wish to acknowledge the financial support received from ANPCYT (PICT 2151 and PIP 292), UNL and CONICET. Thanks are given to Fernanda Mori for the XPS measurements.

Appendix A. Supplementary data

Supplementary data to this article can be found online at https://doi.org/10.1016/j.catcom.2018.05.019.

References

[1] T.S. Moraes, R.C. Rabelo Neto, M.C. Ribeiro, V. Lisiane, M. Mattos, S. Kourtelesis, X. Ladas, F.B. Noronha Verykios, Appl. Catal. B 181 (2016) 754–768.
[2] M. Bilal, S. David Jackson, Appl. Catal. A 529 (2017) 98–107.
[3] T. Hou, B. Yu, S. Zhang, T. Xu, D. Wang, W. Cai, Catal. Commun. 58 (2015) 137–140.
[4] T. van Haasterecht, C.C.I. Ludding, K.P. de Jong, J.H. Bitter, J. Energy Chem. 22 (2013) 257–269.
[5] Y. Mironova, M.M. Ermilova, N.V. Orekhova, D.N. Muraviev, A.B. Yaroslavtsev, Catal. Today 236 (2014) 64–69.
[6] N. Prasongthum, R. Xiao, H. Zhang, N. Tsubaki, P. Natewong, P. Reubroycharoen, Fuel Process. Technol. 160 (2017) 185–195.
[7] D.K. Liguras, D.I. Kondarides, X.E. Verykios, Appl. Catal. B 43 (2003) 345–354.
[8] L. Coronel, J.F. Múnera, A.M. Tarditi, M.S. Moreno, L.M. Cornaglia, Appl. Catal. B 160-161 (2014) 254–266.
[9] A. Karelovic, P. Ruiz, J. Catal. 301 (2013) 141–153.
[10] J.H. Kwak, L. Kovarik, J. Szanyi, ACS Catal. 3 (2013) 2449–2455.
[11] W. Zhen, B. Li, G. Lu, J. Ma, RSC Adv. 4 (2014) 16472–16479.
[12] K.D. Beard, J.W. Van Zee, J.R. Monnier, Appl. Catal. B 88 (2009) 185–193.
[13] M. Bilial, S.D. Jackson, Catal. Sci. Technol. 2 (2012) 2043–2051.
[14] A. Casanovas, J. Llorca, N. Homs, J. Luis G. Fierro, P. Ramírez de la Piscina, J Mol Cat A: Chem 250 (2006) 44–49.
[15] K. Mudiyanselage, I. Al-Shankiti, A. Foulis, J. Llorca, H. Idriss, App. Catal. B 197 (2016) 198–205.
[16] V. Palma, C. Ruocco, F. Castaldo, A. Ricca, D. Boettge, Int. J. Hydrog. Energy 40 (2015) 12650–12662.
[17] M. Compagnoni, A. Tripodi, I. Rossetti, Appl. Catal. B 203 (2017) 899–909.
[18] P.J.L. Gómez de la Fuente, M.V. Martínez-Huerta, S. Rojas, P. Hernández-Fernández, P. Terreros, J.L.G. Fierro, M.A. Peña, Appl. Catal. B 88 (2009) 505–514.
[19] X. Yang, J. Zheng, M. Zhen, X. Meng, F. Jiang, T. Wang, C. Shu, L. Jiang, C. Wang, Appl. Catal. B 121–122 (2012) 57–64.
[20] Y. Liang, J. Li, Q.-C. Xu, R.-Z. Hu, J.-D. Lin, D.-W. Liao, J. Alloys Compd. 465 (2008) 296–304.
[21] C. Carrara, J.F. Múnera, E.A. Lombardo, L.M. Cornaglia, Top. Catal. 51 (2008) 98–106.
[22] J.L.G. de la Fuente, M.V. Martínez-Huerta, S. Rojas, P. Terreros, J.L.G. Fierro, M.A. Peña, Catal. Today 116 (2006) 422–432.